Sucrose phosphorylase from Alteromonas mediterranea : structural insight into the regioselective α-glucosylation of (+)-catechin

Marine Goux, Marie Demonceaux, Johann Hendrickx, Claude Solleux, Emilie Lormeau, Folmer Fredslund, David Tezé, Bernard Offmann, Corinne André-Miral

1 # Sucrose phosphorylase from *Alteromonas mediterranea*: structural

2 # insight into the regioselective α-glucosylation of (+)-catechin

3 Marine Goux[a], Marie Demonceaux[a], Johann Hendrickx[a], Claude Solleux[a], Emilie Lormeau[a], Folmer

4 Fredslund[b], David Tezé[b], Bernard Offmann[a,c] and Corinne André-Miral[a,c]

5

6 [a] Nantes Université, CNRS, US2B, UMR 6286, F-44000, Nantes, France

7 [b] DTU Biosustain, Technical University of Denmark, DK-2800 Kgs. Lyngby, Denmark

8 [c] Corresponding authors: Corinne André-Miral and Bernard Offmann

9 **Abstract**

10 Sucrose phosphorylases, through transglycosylation reactions, are interesting enzymes that can

11 transfer regioselectively glucose from sucrose, the donor substrate, onto acceptors like flavonoids

12 to form glycoconjugates and hence modulate their solubility and bioactivity. Here, we report for

13 the first time the structure of sucrose phosphorylase from the marine bacteria *Alteromonas*

14 *mediterranea* (*Am*SP) and its enzymatic properties. Kinetics of sucrose hydrolysis and

15 transglucosylation capacities on (+)-catechin were investigated. Wild-type enzyme (AmSP-WT)

16 displayed high hydrolytic activity on sucrose and was devoid of transglucosylation activity on (+)-

17 catechin. Two variants, *Am*SP-Q353F and *Am*SP-P140D catalysed the regiospecific

18 transglucosylation of (+)-catechin: 89% of a novel compound (+)-catechin-4′-O-α-D-

19 glucopyranoside (CAT-4') for AmSP-P140D and 92% of (+)-catechin-3′-O-α-D-glucopyranoside

20 (CAT-3') for AmSP-Q353F. The compound CAT-4' was fully characterized by NMR and mass

21 spectrometry. An explanation for this difference in regiospecificity was provided at atomic level by

22 molecular docking simulations: *Am*SP-P140D was found to preferentially bind (+)-catechin in a

mode that favours glucosylation on its hydroxyl group in position 4' while the binding mode in AmSP-Q353F favoured glucosylation on its hydroxyl group in position 3'.

1.   Introduction

Oceans cover more than 70% of Earth's surface and provides a unique environment to marine bacteria (*i.e.* high salinity, high pressure, low temperature and special lighting conditions). For decades, enzymes have been isolated and purified from terrestrial microorganisms, animals and plants. With the advent of biotechnology, there has been a growing interest and demand for enzymes with novel properties and robust biocatalysts. Due to its complexity, the marine environment represents a great opportunity for exploration of new enzymes and molecules [1, 2]. Marine enzymes are capable of being active under extreme conditions, which provide competitiveness and efficiency to different industrial processes [3, 4]. Among those, sucrose-phosphorylases (SPs) from the Glycoside Hydrolase family 13 subfamily 18 (GH13_18, EC 2.4.1.7) attract biotechnological interest as biocatalysts. Requiring only a cheap and abundant donor, SPs can perform transglucosylation reaction by transferring glucose from sucrose to an acceptor to yield α-glucosylated products with a retaining mechanism *via* a β-glucosyl-enzyme intermediate. Particularly, *Bifidobacterium adolescentis* SP (*Ba*SP-WT) and its mutants have been studied for biocatalytic synthesis of rare disaccharides [5, 6] and α-glucosylation of polyphenols [7, 8, 9, 10]. To date, the only documented structures of SP in the literature are from *Bifidobacterium adolescentis* [11]. Other SPs, from *Leuconostoc mesenteroides*, *Streptococcus mutans*, *Lactobacillus acidophilus* and *Thermoanaerobacterium thermosaccharolyticum*, have also been studied for the glucosylation of phenolic compounds [12, 13, 14]. Glucosylation of this type of molecules increases their solubility in water and their bioavailability in health, nutraceuticals and

47 cosmetics applications [15, 16]. Controlling the regioselectivity of this glucosylation is also at stake

48 for the synthesis of new compounds. We recently documented the activity of two variants of

49 *Ba*SP-WT with respect to their ability to transfer regioselectively a glucose moiety onto (+)-

50 catechin as an acceptor substrate [10]. *Ba*SP-Q345F and *Ba*SP-P134D/Q345F glucosylated (+)-

51 catechin on hydroxyl groups in position 3' (OH-3') and 5 (OH-5) with obtainment of three

52 glucosylated regioisomers: (+)-catechin-3′-O-α-D-glucopyranoside (CAT-3'), (+)-catechin-5-O-α-D-

53 glucopyranoside (CAT-5) and (+)-catechin-3',5-O-α-D-diglucopyranoside (CAT-3',5), with a ratio of

54 51:25:24 for *Ba*SP-Q345F and 82:9:9 for *Ba*SP-P134D/Q345F.

55 *Alteromonas mediterranea*, also known as *Alteromonas macleodii* "Deep Ecotype" or AltDE, is an

56 aerobic Gram-negative and mesophilic marine bacterium from the genus of *Proteobacteria* which

57 was first isolated at a depth of 1000 m in the Eastern Mediterranean Sea in 2005 [17, 18, 19]. Wild

58 type form of *Am*SP (*Am*SP-WT) shares 52% of global sequence identity with *Ba*SP-WT. Sequence

59 alignments revealed that both enzymes possess highly conserved regions corresponding to the

60 loop A (*Ba*SP-WT: [336]AAASNLDLYQ[345], *Am*SP-WT: [344]AAASNLDLYQ[353]) and loop B (*Ba*SP-WT:

61 [132]YRPRP[136], *Am*SP-WT: [138]FRPRP[142]) of the catalytic site [20]. In a preliminary screening using

62 homology modelling and molecular docking, we identified that the catalytic cavity of the glucosyl-

63 intermediate of *Am*SP-WT could potentially host a polyphenolic acceptor compound like (+)-

64 catechin. Towards this end, the crystallographic structure of *Am*SP-WT was for the first time

65 recently determined [Goux *et al.*, in preparation]. In the present work, we characterized *Am*SP-WT

66 from a structural and functional perspective, and further analysed its structural and kinetic

67 features. We also investigated the enzymatic properties of two variants of the enzyme towards

68 their propensity to catalyse the regioselective transglucosylation of (+)-catechin. P140D and Q353F

69 mutations, homologous to mutations P134D and Q345F of *Ba*SP-WT, displayed a single transfer

70 reaction product for each enzyme: (+)-catechin-4′-O-α-D-glucopyranoside (CAT-4') for *Am*SP-

71 P140D and CAT-3' for *Am*SP-Q353F. To explain the striking enzymatic activities of those variants,

3

72 we provide in-depth structural insights by docking simulations and modelling. Our results

73 interestingly broaden the available chemo-enzymatic synthetic tools for the efficient regioselective

74 α-glucosylation of polyphenols.

75 **2. Materials and methods**

76 *2.1. Chemicals*

77 (+)-catechin was purchased from Extrasynthèse and PCR primers from Eurofins. All other chemicals

78 were purchased from Sigma-Aldrich or VWR.

79 *2.2. Vector construction and proteins*

80 *Am*SP-WT and its variants were expressed as C-terminally hexahistidine-tagged proteins, allowing

81 affinity purification by standard protocols. *Am*SP-WT gene (UniProt: S5AE64_9ALTE) was ordered

82 from Genscript already cloned in a pET28b vector. Variants *Am*SP-P140D, *Am*SP-Q353F and *Am*SP-

83 P140D/Q353F were obtained by site-directed mutagenesis using primers 1 and 2 for P140D

84 mutation, and primers 3 and 4 for Q353F mutation (Table S1). *E. coli* BL21(DE3) competent cells

85 (Novagen) were transformed and clones were selected using LB-agar medium supplemented with

86 25 µg/mL kanamycin and confirmed by Sanger sequencing (Eurofins Genomics). Proteins were

87 produced, purified and characterized as previously described [10].

88 *2.3. Kinetics of sucrose hydrolysis*

89 All assays were performed in triplicate in 50 mM MOPS-NaOH at pH 8.0 in PCR strip tubes (Axygen)

90 in a total volume of 100 µL at 25°C. Sucrose hydrolysis activities of *Am*SP WT (3 µM) and variants

91 (10 µM) were obtained in the presence of sucrose as donor substrate ranging from 1 mM to 50

92 mM. At 0 and 40 min, 50 µL of reaction volume were sampled and inactivated at 95°C for 5 min.

93 Glucose released due to sucrose hydrolysis was quantified by spectrophotometry thanks to the

enzymatic coupled assay using glucose oxidase and peroxidase (GOD-POD), and 2,2'-azino-bis(3-ethylbenzothiazoline-6-sulfonic acid (ABTS) as chromogenic peroxidase substrate. In a 96-well plate, a volume of 25 µL of each sample were added to 200 µL of ABTS solution [5 mg/mL ABTS, 5 mg/mL glucose oxidase, 5 mg/mL peroxidase, 30 mM citrate buffer-NaOH pH 6.0]. Plates were incubated for 10 min at 25°C inside a Labsystems integrated EIA Management System and absorbance was measured at 405 nm. Kinetic data were fitted to Michaelis-Menten non-linear model and Hanes-Woolf linear model using respectively *nlm* and *lm* functions implemented in R to estimate the kinetic parameters (Figure S3 and S4, Table 1).

2.4.   Kinetics of the transglucosylation

Reactions were carried out in 50 mM MOPS-NaOH solution at pH 8.0 in a total volume of 1 mL. Reaction mixture containing 10 mM (+)-catechin in DMSO (1 eq., 100 µL), 20% DMSO (100 µL, (v/v)), 80 mM sucrose in H_2O (8 eq., 100 µL) was incubated with a final concentration of 10 µM of purified enzyme at 25°C under slight agitation. Enzymatic synthesis was monitored by thin layer chromatography (TLC) for 24h. TLC plates were developed in solution composed of ethyl acetate/methanol/cyclohexane/water (7:1.5:1:1, v/v/v/v) with 0.1% formic acid (v/v). Products were visualized using a UV lamp at 254 nm and revealed with vanillin-sulphuric acid reagent. After centrifugation (ThermoScientific, Heraeus Pico17 Centrifuge, rotor 75003424, 20 min, 12 000g, 20°C), supernatant of the enzymatic reaction medium was analysed by analytical HPLC at 280 nm on a C-18 column (Interchim, 5µm, 250 x 4.6 mm, US5C18HQ-250/046) with an isocratic flow of 80% H2O, HCOOH 0.1% (v/v) and 20% MeOH, HCOOH 0.1% (v/v) for 20 min. Compound concentrations were calculated from the area under the curves obtained by analytical HPLC on a C-18 column. The assay was performed in triplicate.

116   *2.5.   Purification and analysis of glucosylated (+)-catechin*

117   After 24h of incubation at 25°C under slight agitation, reaction media was centrifuged (12 000 g, 20

118   min) and supernatant was purified by HPLC at 280 nm on a C-18 column (Interchim, 5 µm, 250 x

119   21.2 mm, US5C18HQ-250/212) with a gradient system (solvent A: H2O HCOOH 0.1%; solvent B:

120   MeOH, HCOOH 0.1%; t0 min = 70/30, t10 min = 70/30, t70 min = 10/90). Products were identified

121   by mass spectroscopy (H$^-$ mode, Waters, UPLC-MS2 high resolution) and NMR ^{1}H and ^{13}C in DMSO-

122   d$_6$ (Bruker, Pulse 400 MHz RS2D, 256 scans). Chemical shifts are quoted in parts per million (ppm)

123   relative to the residual solvent peak. Coupling constant J are quoted in Hz. Multiplicities are

124   indicated as d (doublet), t (triplet), m (multiplet). NMR peak assignments were confirmed using 2D

125   ^{1}H correlated spectroscopy (COSY), 2D ^{1}H nuclear Overhauser effect spectroscopy (NOESY) and 2D

126   ^{1}H-^{13}C heteronuclear single quantum coherence (HSQC). Complete characterization of CAT-4' is

127   provided in the ESI, for CAT-3', CAT-5 and CAT-3',5, please see [10].

128

129   *2.6.   Docking analysis of binding mode of (+)-catechin in the catalytic pocket*

130   All docking experiments were performed with AutoDock Vina using, for each variant of the

131   enzyme, 50 models of its glucosyl-intermediate form built using Rosetta suite of software [22] and

132   12 (+)-catechin conformers (see Electronic Supplementary Information for details of the

133   modelling). Docking perimeter was limited to the residues of the active site of the enzyme. Each of

134   the 12 conformers of (+)-catechin were docked on every conformer of the two variants of AmSP.

135   This amounts to a total of 600 (50x12) docking experiments for each variant of the enzyme. Only

136   the productive poses that could lead to a glucosylation of (+)-catechin were selected. To do so,

137   docking poses were filtered using the following distance constraints: distances within 3.0 Å

138   between any oxygen of (+)-catechin and the anomeric carbon atom C1 of the glucosyl moiety were

139 assessed. Docking scores were compiled for these productive poses and compared between the

140 two variants.

3. Results

3.1. Highly conserved structural features and potential activity of AmSP-WT

143 Through structural comparison of *Ba*SP-WT (PDB: 1R7A, 2GDV), *Ba*SP-Q345F (PDB: 5C8B), and our

144 recently determined structure of *Am*SP-WT (PDB: 7ZNP), we identified the conserved residues

145 likely involved in the reaction mechanism and potential substrate interactions (Table S2~~1~~). The −1

146 subsite of SPs, also called donor site, has an optimal topology for binding glucose and is conserved

147 between *Ba*SP-WT and *Am*SP-WT (Figure 1). The configuration of the two catalytic residues

148 involved in the reaction mechanism are also almost identical (Figure 1A, in blue): a glutamyl

149 residue acts as a general acid/base catalyst (E243 for *Am*SP-WT and E232 for *Ba*SP-WT) and an

150 aspartyl residue performs the nucleophilic attack (D203 for *Am*SP-WT and D192 for *Ba*SP-WT). The

151 third member of the catalytic triad (D301 for *Am*SP-WT and D290 for *Ba*SP-WT) stabilises the

152 transition state with a strong hydrogen bond and presents also an identical configuration in the

153 catalytic site. The structural elements that were shown to stabilize the glucosyl moiety in *Ba*SP-WT

154 by non-polar contacts between a hydrophobic platform (F53/F156 for *Ba*SP-WT) and the

155 hydrophobic C3-C4-C5 part of glucose are also conserved in *Am*SP-WT (F56/F167). The acceptor or

156 +1 site of SPs is mainly shaped by two highly dynamic loops (Figure S1), which were shown to

157 adopt different conformations based on the progress of the reaction mechanism: one

158 conformation is the "donor binding mode" or closed conformation and the other is the "acceptor

159 binding mode" or open conformation where an arginyl residue (R135 in *Ba*SP-WT) is thought to

160 enable the enzyme to outcompete water as an acceptor through strong electrostatic interactions.

161 When we compare the apoenzyme of *Ba*SP-WT (PDB: 1R7A) with our newly obtained apoenzyme

of *Am*SP-WT (PDB: 7ZNP), a striking difference in the positioning of loop A is noticed. The enzyme has already an opened conformation and is in the "acceptor binding mode" with Y352 residue pointing inside the active site (Figure 1, in magenta) and R141 pointing outside (Figure 1, in orange). This open conformation was also observed for *Ba*SP-WT crystallized with the end-product of the reaction after hydrolysis of glucose (PDB: 2GDV, chain B). Moreover, crucial conserved residues involved in binding of both phosphate and fructose, Y196 and H234 for *Ba*SP-WT *vs.* Y207 and H245 for *Am*SP-WT, are in the same conformational positions thus allowing sucrose phosphorylase activity (Figure 1B, in cyan)[21]. In *Ba*SP-WT, Y132 is located at the entrance of the active site and contributes to sucrose specificity thanks to hydrophobic interactions with Y196 and F206. In *Am*SP-WT, the aromatic structure is conserved with the replacement of the tyrosinyl moiety by a phenylalanyl residue in position 138 (Figure 1B, in orange).

3.2.   Determination of the apparent kinetic parameters for sucrose hydrolysis

C-terminally hexahistidine-tagged *Am*SP-WT and variants were produced in BL21(DE3) and purified by Ni-NTA immobilized metal affinity chromatography for further characterization. Interestingly, the P140D and Q353F mutations did not alter the enzyme stability, as evidenced by unchanged melting temperature (T_m) of 43°C (Figure S2, Table S3). The apparent kinetic parameters for sucrose hydrolysis at 25°C were determined (Table 1). Globally, AmSP-WT has a higher apparent affinity towards sucrose (lower Km value) and higher turn-over number (kcat) than the studied variants. Lower activity for sucrose hydrolysis could be indicative of potential increased capacity in transglucosylation. For *Am*SP-WT, DMSO did not change significantly the K_m and *kcat* values. Interestingly, for the P140D and Q353F mono-variants, the presence of DMSO 20% increased the *kcat* two-fold and its specificity constant (*kcat/Km*) about 4-fold with respect to absence of co-solvent. With respect to the wild-type enzyme, in presence of DMSO, *Am*SP-P140D displayed a similar affinity for sucrose similar but a turnover number divided by almost 3-fold, leading to a

186 kinetic efficiency (*kcat/Km*) divided by two. In the same conditions, *Am*SP-Q353F (Km = 2 mM) has

187 a two fold decrease in affinity with respect to AmSP-WT (K_m =1 mM) and a corresponding 19-fold

188 decrease in its turnover number.

189 *3.3.   (+)-catechin transglucosylation studies*

190 We assessed the ability of SPs to transfer a glucose moiety from sucrose to (+)-catechin at 25°C

191 after 24h under agitation (Figure S3). Observed products were purified by preparative HPLC and

192 analysed by NMR and mass spectrometry. *Am*SP-P140D and *Am*SP-Q353F catalyse efficiently the

193 synthesis of two different regioisomers of (+)-catechin glucoside: *Am*SP-P140D glucosylated mostly

194 the hydroxyl groups in position 4' (OH-4') while *Am*SP-Q353F glucosylated the OH-3' position

195 (Figures S5B and S5C, Table S4). We monitored the synthesis of glucosylated (+)-catechin products

196 during 24h by HPLC to determine conversion yields and proportion of regioisomers (Figure 2, Table

197 2). Interestingly, the main product formed with *Am*SP-P140D was CAT-4' with a relative proportion

198 of 89% while the main product formed with AmSP-Q353F was CAT-3' with a relative proportion of

199 92%. The corresponding synthetic yields (percentage of (+)-catechin that was converted into these

200 glycosylated products) was 26% and 82% respectively. These results clearly indicate that these

201 two variants are highly regioselective with respect to their transglycosylation activities on (+)-

202 catechin.

203 *3.4.   Structural insights into the regioselectivity of AmSP-P140D and AmSP-Q353F*

204 To further understand the observed regioselectivities, we performed molecular docking

205 simulations on *Am*SP-Q353F and *Am*SP-P140D. The preferred orientations of (+)-catechin in the

206 acceptor site of the glucosyl-enzyme intermediate were assessed. Docking results were consistent

207 with the observed experimental regioselectivity. For *Am*SP-Q353F, binding mode of(+)-catechin

208 suggest preference for transglycosylation in OH3' position (Figures 3 and S7). On the other hand,

209 for *Am*SP-P140D, the binding mode of (+)-catechin suggest preference for transglycosylation in

210 OH-4' position (Figures 3 and S7). For *Am*SP-P140D, (+)-catechin is stabilized in the active +1 site

211 by a network of 4 hydrogen bonds and numerous hydrophobic contacts (Figure 4).

4.   Discussion

213 In glycochemistry, the fine control of the regioselectivity is the Holy Grail in enzymatic reactions

214 catalysed by glycosyl hydrolase (GHs) such as sucrose phosphorylase. A disadvantage of GHs is

215 their moderate regioselectivity, meaning that a mixture of products is often formed when the

216 acceptor contains more than one hydroxyl group. Previously, for (+)-catechin which consists of five

217 phenolic hydroxyl groups, we generated with *Ba*SP-Q345F and *Ba*SP-P134D/Q345F a mixture of

218 glucosylated regioisomers: CAT-3', CAT-5 and CAT-3',5 with a ratio of 51:25:24 for *Ba*SP-Q345F and

219 82:9:9 for *Ba*SP-P134D/Q345F. Another drawback is the relatively low product yields. With the

220 same variants, we obtained a synthetic yield of 34%/15%/9% and 40%/5%/4%, respectively. In the

221 active site of the SPs, the −1 site is rigid to allow a high selectivity on glucose while the +1 site is

222 more flexible and can accept several types of acceptors or leaving groups. The +1 site of *Am*SP-WT,

223 is mainly shaped by two highly labile loops, loop A (³⁴⁴AAASNLDLYQ³⁵³) and loop B (¹³⁸FRPRP¹⁴²),

224 which undergo crucial conformational changes throughout the catalytic cycle suited for binding

225 either fructose or phosphate. Crystal structure of *Am*SP-WT shows a wide access channel capable

226 of accommodating naturally large polyphenolic acceptors. We decided to perform homologous

227 mutations as what was done on *Ba*SP to check their impact on regioselectivity in the context of

228 *Am*SP. By site-directed mutagenesis, we hence substituted the residue Q353 in loop A into F353

229 and/or the residue P140 into D140 in Loop B. We obtained three variants: *Am*SP-P140D, *Am*SP-

230 Q353F and *Am*SP-P140D/Q353F. The double variant showed no improvement for the synthesis of

231 CAT-3' with the obtainment of a mixture of products at 25°C (Figure S5D) and was not further

232 characterized.

234 By engineering only the residue 353 of the active site, we obtained an enhanced regioselectivity

235 with glucosylation at OH-3' position almost exclusively (Figure S5B). Interestingly, we also noticed

236 that transglucosylation is most favored for this variant compared to hydrolysis in presence of (+)-

237 catechin. Indeed, transglucosylation reaction proceeded to nearly completion within 24h (Figure 2)

238 for AmSP-Q353F while rate of sucrose hydrolysis was very low (Table 1). *Am*SP-Q353F, as it was

239 shown for *Ba*SP-Q345F and *Ba*SP-P134D/Q345F, preferentially glucosylate the OH-3' position of

240 flavonoids while ignoring the OH-4' position. Docking studies confirmed that the most favoured

241 pose for (+)-catechin in the catalytic +1 site of AmSP-Q353F lead to the formation of CAT-3' (Figure

242 3A and 3C, and Table 2). As seen with BaSP-Q345F, we hypothesized that the introduction of F353

243 as a potential partner for π–π stacking would lead to rearrangements in loop A with a shift of Y352

244 which could stabilize (+)-catechin in the active site by hydrophobic interactions (Figures 4B and

245 S8).

246 Surprisingly, while BaSP-P140D was not active, *Am*SP-P140D leads to the regioselective formation

247 of CAT-4' (Figure S5C and Table 2). Thus, the regioselectivity of *Am*SP shifted completely from CAT-

248 3' in Q353F variant to CAT-4' in P140D variant. An explanation enlightened by molecular modelling

249 is the steric hindrance caused by F138/Y207/F217 residues in AmSP-P140D that does not favor

250 orientation of the substrate for CAT-3' synthesis (Figures 3A, 3B and S8). Indeed, we observed that

251 the conformation of the acceptor site drastically changed and seems to allow only an almost linear

252 orientation of all three (+)-catechin rings (Figure S8). Contrarily to AmSP-Q353F, those very strong

253 constraints lead to the regioselective glucosylation of the OH-4' position of the flavonoid with a

254 high proportion (89%). However, as shown in Figure 2, overall yield does not exceed 26% for the

255 CAT-4' transglucosylation product. We hypothesized that it is mainly due to the possible

256 competition between (+)-catechin, sucrose and water into the active site, favoring the sucrose

257 hydrolysis reaction (Figures S3 and S4).

5.   Conclusion

In this study, we provided the first report of the use of variants of sucrose phosphorylase from *Alteromonas mediterranea* for the regioselective transglucosylation of (+)-catechin and the synthesis of a novel compound fully characterized, (+)-catechin-4′-O-α-D-glucopyranoside (CAT-4'). *Am*SP-Q353F and *Am*SP-P140D are able to synthesize regioselectively compound CAT-3' and CAT-4', with a proportion of 92% and 89%, respectively. With *Am*SP-P140D, we succeed to switch the regioselectivity from OH-3' to OH-4'-glucosylated (+)-catechin. Mutation P140D changes drastically the conformation of the acceptor site and seems to allow an almost linear alignment of the glucose moiety and of all three (+)-catechin rings allowing selectively the glucosylation of the position OH-4' of this flavonoid. Overall, the results described herein suggest that *Am*SP-Q353F and *Am*SP-P140D are suitable for the enzymatic regioselective synthesis of polyphenolic glucosides at high yields and could facilitate the synthesis of *de novo* products in OH-4' position using other phenolic phytochemicals such as quercetin or kaempferol.

Supporting information

Details about AmSP-WT sequence, primers, melting curves, kinetic parameters analysis, transglucosylation studies, HPLC/MS and NMR spectra are provided in the Electronic Supplementary Information.

Author Contributions

MG and MD wrote the original draft. MG, MD, CM, BO and JH developed the methodology. MG, MD, CS and EL performed the experimental investigation and the subsequent analysis. DT and FF obtained the crystallographic structure of *Am*SP-WT. JH and BO performed the molecular and

docking simulations and the following analysis. CM obtained the funding, designed and directed the project. All authors discussed the results and contributed to the final manuscript.

Conflicts of interest
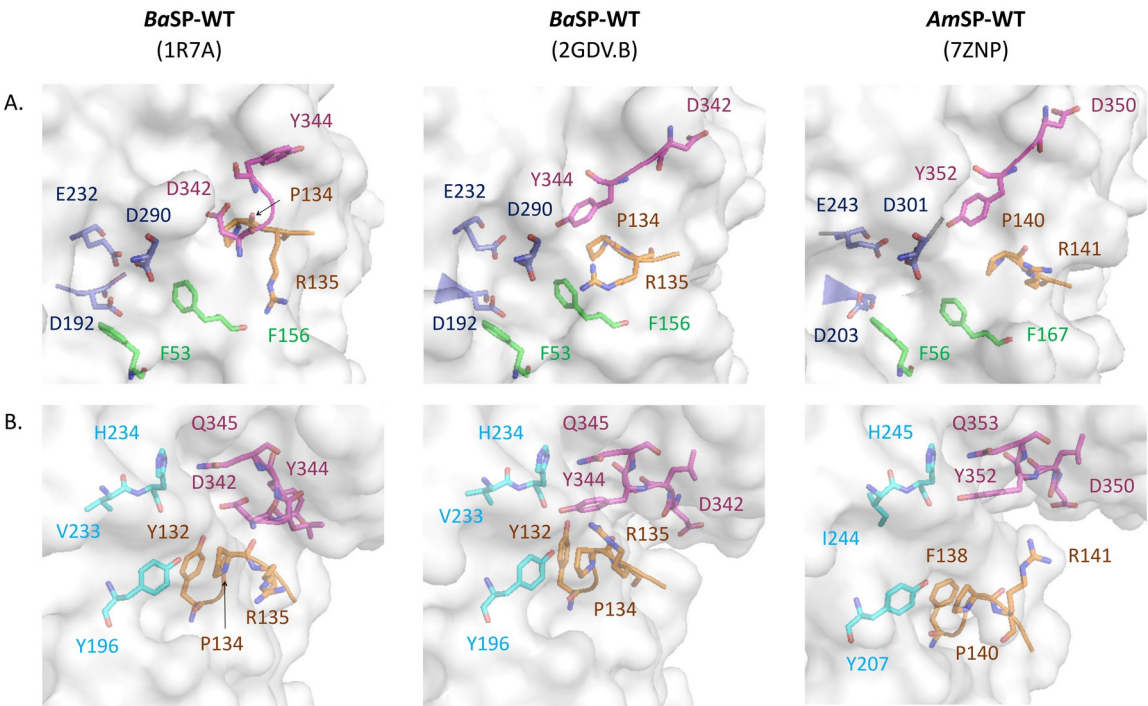
There are no conflicts to declare.

References

[1] A. Beygmoradi, A. Homaei, R. Hemmati, Marine chitinolytic enzymes, a biotechnological treasure hidden in the ocean?, Appl. Microbiol. Biotechnol. 102 (2018) 9937–9948. https://doi.org/10.1007/s00253-018-9385-7

[2] V.S. Bernan, M. Greenstein, M.W. Maiese, Marine microorganisms as a source of new natural products, Adv. Appl. Microbiol. 43 (1997) 57-90. https://doi.org/10.1016/s0065-2164(08)70223-5.

[3] H. Harmsen, D. Prieur, C. Jeanthon, Distribution of microorganisms in deep-sea hydrothermal vent chimneys investigated by whole-cell hybridization and enrichment culture of thermophilic subpopulations, Appl. Environ. Microbiol. 63 (1997) 2876-2883. https://doi.org/10.1128/aem.63.7.2876-2883.1997.

[4] T.H. Cheng, N. Ismail, N. Kamaruding, Industrial enzymes-producing marine bacteria from marine resources, Biotechnology Reports. 27 (2020) e00482. https://doi.org/10.1016/j.btre.2020.e00482.

301   [5]   M. Kraus, J. Görl, M. Timm, Synthesis of the rare disaccharide nigerose by structure-based

302   design of a phosphorylase mutant with altered regioselectivity, ChemComm 52 (2016)

303   4625–4627. https://doi.org/10.1039/c6cc00934d.

304   [6] J. Franceus et al., "Rational design of an improved transglucosylase for production of the

305   rare   sugar   nigerose,   ChemComm.   55   (2019)   4531–4533.

306   https://doi.org/10.1039/c9cc01587f.

307   [7] M. Kraus, C. Grimm, J. Seibel, Redesign of the Active Site of Sucrose Phosphorylase through

308   a   Clash-Induced   Cascade   of   Loop   Shifts,   ChemBioChem   17   (2016)   33–36.

309   https://doi.org/10.1002/cbic.201500514.

310   [8] M. Kraus, C. Grimm, J. Seibel, "Switching enzyme specificity from phosphate to resveratrol

311   glucosylation, ChemComm. 53 (2017) 12181–12184. https://doi.org/10.1039/c7cc05993k.

312   [9] D. Aerts, T. F. Verhaeghe, B. I. Roman, Transglucosylation potential of six sucrose

313   phosphorylases toward different classes of acceptors, Carbohydr. Res. 346 (2011) 1860-

314   1867. https://doi.org/10.1016/j.carres.2011.06.024.

315   [10]   M. Demonceaux, M. Goux, M., J. Hendrickx, Regioselective glucosylation of (+)-

316   catechin using a new variant of the sucrose phosphorylase from *Bifidobacterium*

317   *adolescentis*, Org. Biomol. Chem. 11 (2023). https://doi.org/10.1039/d3ob00191a.

318   [11]   D. Sprogoe, L.A.M. van den Broek, O. Mirza, Crystal structure of sucrose

319   phosphorylase from Bifidobacterium adolescentis, Biochemistry 43 (2004) 1156-1162.

320   https://doi.org/10.1021/bi0356395.

321   [12]   M. E. Dirks-Hofmeister, T. Verhaeghe, K. De Winter, Creating Space for Large

322   Acceptors: Rational Biocatalyst Design for Resveratrol Glycosylation in an Aqueous System,

323   Angew. Chemie. 54 (2015) 9289–9292. https://doi.org/10.1002/anie.201503605.

324 [13] S. Kitao, T. Ariga, T. Matsudo, The Syntheses of Catechin-glucosides by

325 Transglycosylation with Leuconostoc Mesenteroides Sucrose Phosphorylase, Biosci.

326 Biotechnol. Biochem. 57 (1993). 2010–2015, 1993, https://doi.org/10.1271/bbb.57.2010.

327 [14] K. De Winter, G. Dewitte, M.E. Dirks-Hofmeister, Enzymatic Glycosylation of

328 Phenolic Antioxidants: Phosphorylase-Mediated Synthesis and Characterization, Journal of

329 Agricultural and Food Chemistry 2015 63 (46) 10131-10139.

330 https://doi.org/10.1021/acs.jafc.5b04380

331 [15] K. De Winter, A. Cerdobbel, W. Operational stability of immobilized sucrose

332 phosphorylase: continuous production of α-glucose-1-phosphate at elevated

333 temperatures. Process Biochem. 46 (2011) 1074–1078.

334 https://doi.org/10.1016/j.procbio.2011.08.002.

335 [16] J. Franceus, T. Desmet, Sucrose Phosphorylase and Related Enzymes in Glycoside

336 Hydrolase Family 13: Discovery, Application and Engineering, Int. J. Mol. Sci. 21 (2020)

337 2526. https://doi.org/10.3390/ijms21072526

338 [17] A. López-López, S.G. Bartual, L. Stal, Genetic analysis of housekeeping genes reveals

339 a deep-sea ecotype of Alteromonas macleodii in the Mediterranean Sea, Environ Microbiol.

340 7 (2005)649-659. https://doi.org/10.1111/j.1462-2920.2005.00733.x

341 [18] E.P. Ivanova, M. López-Pérez, M. Zabalos, Ecophysiological diversity of a novel

342 member of the genus Alteromonas, and description of Alteromonas mediterranea sp. nov.

343 Antonie Van Leeuwenhoek. 107 (2015) 119-132. https://doi.org/10.1007/s10482-014-

344 0309-y

345 [19] M. López-Pérez, A. Gonzaga, A.B. Martin-Cuadrado, Genomes of surface isolates of

346 Alteromonas macleodii: the life of a widespread marine opportunistic copiotroph. Sci Rep

347 2, 696 (2012). https://doi.org/10.1038/srep00696

348   [20]   O. Mirza, L.K. Skov, D. Sprogoe, Structural Rearrangements of Sucrose

349   Phosphorylase from Bifidobacterium adolescentis during Sucrose Conversion, J. Biol. Chem.

350   281 (2006) 35576-35584. https://doi.org/10.1074/jbc.M605611200.

351   [21]   T. Verhaeghe, M. Diricks, D., Mapping the acceptor site of sucrose phosphorylase

352   from Bifidobacterium adolescentis by alanine scanning, J. Mol. Catal 96 (2013) 81-88.

353   https://doi.org/10.1016/j.molcatb.2013.06.014

354   [22]   C. A. Rohl, C.E. Strauss, K.M. Misura, Protein structure prediction using Rosetta,

355   Methods Enzymol. 383 (2004) 66–93. https://doi.org/10.1016/S0076-6879(04)83004-0

356   [23]   R. Schumacker and S. Tomek, Understanding Statistics Using R, Springer, 2013.

357   https://doi.org/10.1007/978-1-4614-6227-9

358   [24]   R. A. Laskowski, M. B. Swindells, LigPlot+: multiple ligand-protein interaction

359   diagrams for drug discovery. J. Chem. Inf. Model., 51 (2011) 2778-2786.

360   https://doi.org/10.1021/ci200227u

361

Figures caption and legend

Figure 1: Crystallographic structures of *Ba*SP-WT and *Am*SP-WT focused on residues involved in (A) sucrose and (B) fructose binding. (A) In magenta: Loop A (in sticks for *Ba*SP-WT: Y344/D342, in sticks for *Am*SP-WT: Y352/D350); orange: Loop B (in sticks for *Ba*SP-WT: R135, in sticks for *Am*SP-WT: R141); green: hydrophobic platform (in sticks for *Ba*SP-WT: F53 and F156, in sticks for *Am*SP-WT: F56 and F167); and blue: residues of the catalytic triad (in sticks for *Ba*SP-WT: D192/E232/D290, in sticks for *Am*SP-WT: D203/E243/D301). **(B)** In magenta: Loop A (in sticks for *Ba*SP-WT: D342/L343/Y344/Q345, i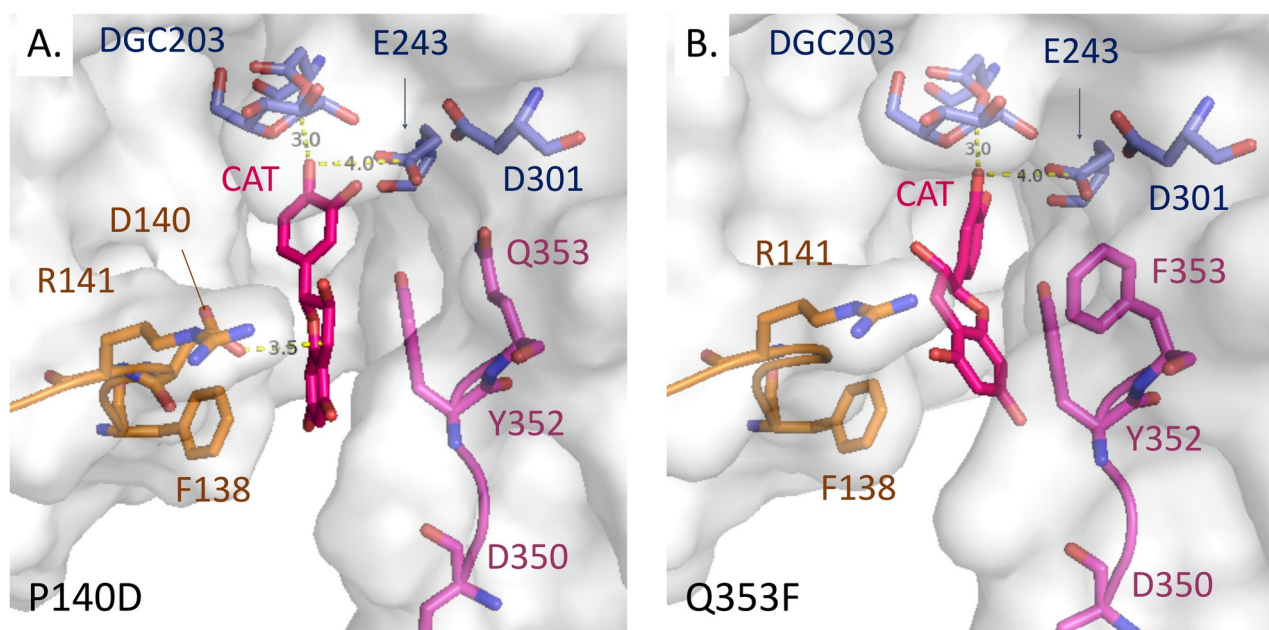n sticks for *Am*SP-WT: D350/L351/Y352/Q353); orange: Loop B (in sticks for *Ba*SP-WT: Y132/R133/P134/R135, in sticks for *Am*SP-WT: F138/R139/P140/R141); Cyan: residues involved in sucrose phosphorylase activity (in sticks for *Ba*SP-WT: Y196/V233/H234, in sticks for *Am*SP-WT: Y207/I244/H245).

Figure 2: Products profile of AmSP-Q353F and AmSP-P140D using (+)-catechin as acceptor. Compound concentrations were calculated from the area under the curves obtained by analytical HPLC on a C-18 column for 7h and at 2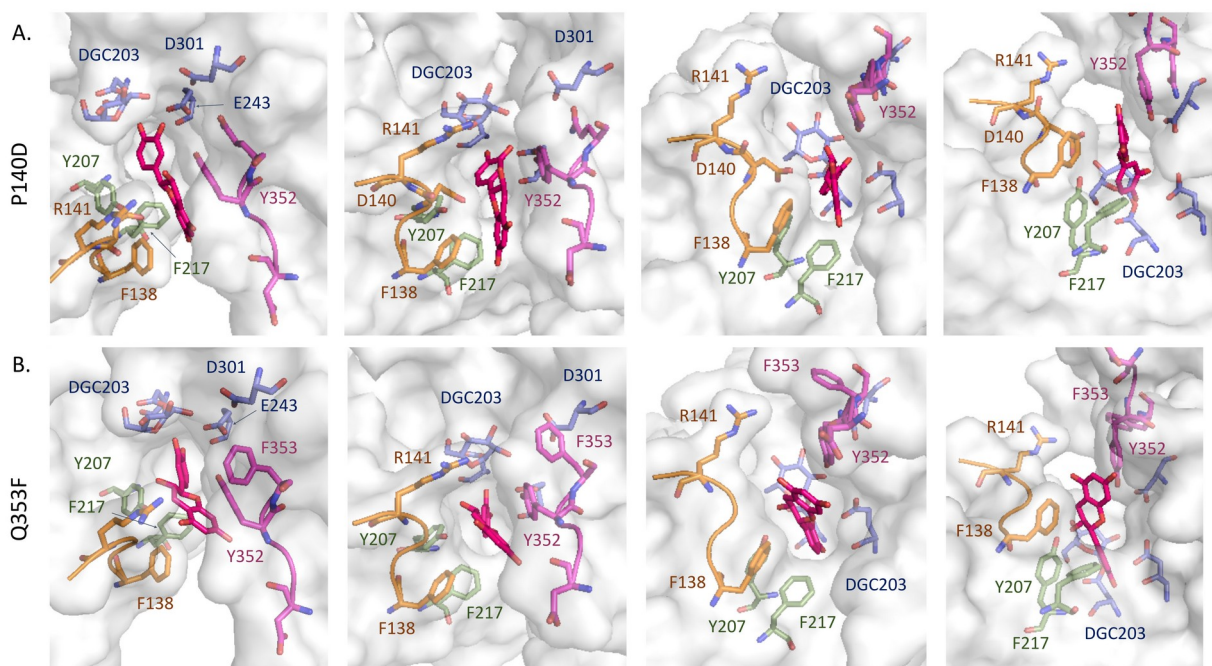4 h of incubation at 25°C of the reaction mixture in a final volume of 1 mL in MOPS-NaOH 50 mM pH 8.0 with 10 µM of enzyme, 80 mM sucrose and 20% DMSO (v/v) (n=3). Errors correspond to standard deviations. Details of the data can be found in ESI (Table S4).

18

Figure 3: Comparison of the binding mode of (+)-catechin in AmSP-P140D and AmSP-Q353F. (A) Best binding mode of (+)-catechin in AmSP-P140D glucosyl-enzyme intermediate. (B) Best binding mode of (+)-catechin in AmSP-Q3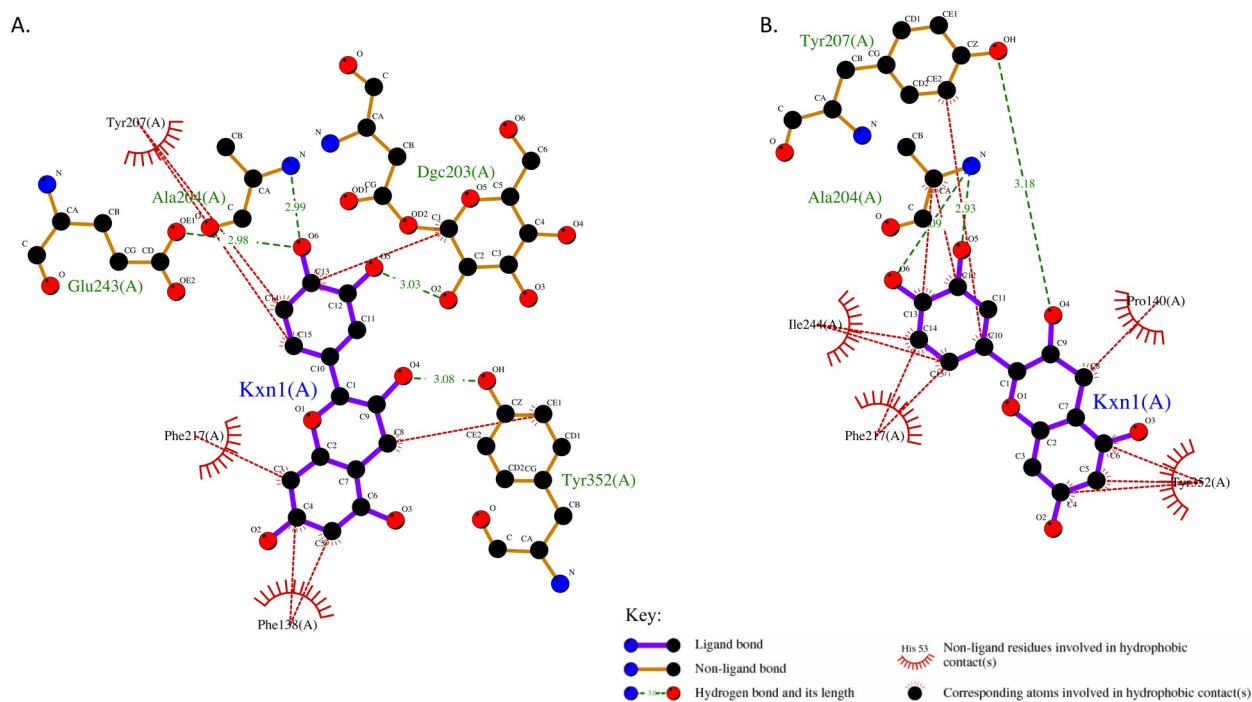53F glucosyl-enzyme intermediate. In magenta, loop A with in sticks Y352/D350/Q(F)353 residues; in orange, loop B in orange with in sticks R141/F138 and D140 for AmSP-P140D; in blue, residues of the catalytic triad with in sticks DGC203/E243/D301; in pink, (+)-catechin.

394

Figure 4. Analysis of the interaction between (+)-catechin and AmSP variants. Shown are hydrogen bonds and representative hydrophobic contacts between the (+)-catechin substrate (denoted Kxn1) and the interacting residues including the glucosylated-aspartyl (DGC203) in (A) AmSP-P140D and (B) AmSP-Q353F. The diagram was obtained using LigPlot Plus v.2.2 [24].

399

400

Table 1: Apparent kinetic parameters for sucrose hydrolysis by AmSP and its variants.

Data were obtained by glucose titration using GOD/POD method of the reaction medium that reacted for 3h at 25°C and that contained the SP enzyme (10 µM for variants and 3 µM for WT) and 1 mM to 50 mM of sucrose, in MOPS-NaOH 50 mM pH 8.0 (n=3). Values are based on linear fit to the Hanes-Woolf model. Michaelis-Menten and Hanes-Woolf plots are provided in the ESI (Figures S3 and S4).

	0% DMSO			20% DMSO		
	K_M (mM)	k_{cat} (min^{-1})	k_{cat}/K_M	K_M (mM)	k_{cat} (min^{-1})	k_{cat}/K_M
*Am*SP-WT	1.3	56.9	42.8	1.5	68.4	46.9
*Am*SP-P140D	2.2	14.7	6.7	1.0	24.3	24.1
*Am*SP-Q353F	7.1	3.0	0.4	2.3	5.6	2.5
*Am*SP-P140D/Q353F	12.6	2.1	0.2	6.9	1.1	0.2

407

408

409 **Table 2: Synthetic yields (A) and relative proportion (B) of (+)-catechin glycosylated products**

410 **obtained with P140D and Q353F variants of AmSP.** Synthetic yields and relative proportions of

411 each product are expressed as a percentage of (+)-catechin that was converted into the

412 corresponding glycosylated products (CAT-4': (+)-catechin-4′-O-α-D-glucopyranoside; CAT-3':

413 (+)-catechin-3′-O-α-D-glucopyranoside; CAT-5: (+)-catechin-5-O-α-D-glucopyranoside; CAT3',5:

414 (+)-catechin-3',5-O-α-D-diglucopyranoside). The relative proportion of each product was calculated

415 from the area under the curves obtained by analytical HPLC at 24 h with the same conditions than

416 for Figure S5. Values were obtained from the area under the curves obtained by analytical HPLC of

417 the reaction mixture containing 10 μM enzyme, 10 mM (+)-catechin, 80 mM sucrose, 20% DMSO

418 (v/v) in MOPS 50 mM pH 8.0, and incubated at 25°C for 24 h. Details of the data can be found in

419 ESI (Table S4, Figure S5).

Product	Synthetic yields				Proportion of each product			
	CAT-4'	CAT-3'	CAT-5	CAT-3',5	CAT-4'	CAT-3'	CAT-5	CAT-3',5
P140D	26%	3%	Traces	Traces	89%	11%	Traces	Traces
Q353F	3%	83%	2%	2%	4%	92%	2%	2%

420